Journal of Information Technology Management

Print ISSN: 2008-5893

Online ISSN: 2423-5059

Design and Characterization of a Low-Cost Capacitive Soil Moisture Sensor System for IoT based Agriculture Applications

Siddhanta Borah

Department of Electronics and Instrumentation Engineering, National Institute of Technology Nagaland, Nagaland, India. E-mail: borahsidd@gmail.com

R. Kumar*

*Corresponding Author, Department of Electronics and Instrumentation Engineering, National Institute of Technology Nagaland, Nagaland, India. E-mail: rajagopal.kumar4@gmail.com

Subhradip Mukherjee

Department of Electronics and Instrumentation Engineering, National Institute of Technology Nagaland, Nagaland, India. E-mail: subhradip11@gmail.com

Abstract

The global demand for food can be eliminated by precision farming. This research work proposes a low-cost IoT-enabled handy device to measure soil water content. Three different sensor probes are designed in COMSOL Multiphysics 5.4 and fabricated using PCB Technology. The designed sensor probes are calibrated to effectively measure moisture content for three different soil types (silt/sandy/clay). An electronic system has been programmed according to Optimized-Moisture-Value (OMV) algorithm to read and collect the soil moisture information. Three sensor probes, capacitance, and voltage responses are analyzed using linear fitting. It has been observed from the response data that model B's performance is better than the other two presented models in terms of soil moisture. The obtained goodness of fitness value for model B is around 0.999 for all the categories of soils. The electronic system is built around W78E054D and ESP8266 controllers. The W78E054D controller is used to excite the sensor probe with a signal having a frequency of 500 kHz. The IoT-enabled controller ESP8266 reads and collects the soil moisture data according to the OMV algorithm.

Keywords: Fringing field capacitive sensor; Soil moisture; Internet of Things (IoT); OMV algorithm; COMSOL simulation.

Journal of Information Technology Management, 2023, Vol. 15, Special Issue, pp. 95-111
Published by University of Tehran, Faculty of Management
doi: https://doi.org/ 10.22059/jitm.2023.91570
Article Type: Research Paper

Received: December 22, 2022
Received in revised form: January 15, 2023
Accepted: February 20, 2023
Published online: March 15, 2023

Introduction

For precision agriculture, measuring soil water content is crucial to control irrigation. Irrigation depends on many other environmental factors, such as environmental temperature, humidity, and soil type (Bao et al., 2016; Uddin et al., 2016; Tang Chunling & Chen Dong, 2017). To measure soil moisture content, different types of sensors are available. Most such sensors are resistive. Capacitive sensors are more influential and long-lasting since the sensor probe does not directly come in contact with dry/wet soil, a capacitive sensor system and the capacitance changes due to the change of dielectric medium between two capacitive plates. Over the last two decades, researchers have been working on capacitive sensors to measure soil water content. Mainly three different types of water are present in the soil (Lekshmi et al., 2014; Raats & Genuchten, 2006). The content of gravitational water usually is shallow in the soil. It drains out quickly due to gravitational force. The content of such water depends on the type of soil. Capillary water is usually found in most soil due to capillary action. Very tiny particles of soil absorb water. Hygroscopic water is present in the air. So, such water usually is present on the surface of the soil. Clayey soil can hold more water than sandy soil since sandy soil has less surface area.

Different strategies are used to measure the content of such water in the soil. Some of the well-known strategies are ground penetrating radar (Huisman et al., 2003), time domain reflectometry (Ledieu et al., 1986; Rao & Singh, 2011), frequency domain reflectometry (Lin, 2003; Minet et al., 2010), optical techniques (Alessi & Prunty, 1985; Scott 2003), neutron scattering techniques (Evett & Steiner, 1995), gamma scattering techniques (Zazueta & Xin, 1994). Among all these techniques, TDR and FDR techniques are mostly preferred to find the moisture content in the soil. There is a drastic dielectric constant change between wet soil (Approximately 70-80) and dry soil (Approximately 2-4). Hence, an apparent variation in the output is observed in measuring water content in the soil.

Fringing field capacitive sensors are the perfect examples of measuring soil water content based on a dielectric medium between the two electrodes. Sophisticated Micro Electro Mechanical System (MEMS) based fringing field sensors have many applications. Some studies show how such sensor systems are used to detect the movement of objects (Thamaraimanalan et al., 2010; Langfelder & Tocchio, 2012). Hence some change in the output is obtained. A MEMS-based soil moisture sensor is presented. (Chen & Luo, 1998).

Their design shows that the sensor size cannot determine sensor output. Besides, it depends on the geometrical structure of the MEMS sensor. Moreover, some studies show that the output of capacitive soil sensors is highly dependent on the dielectric medium of the capacitor (Curtis, 2001; Ritchey, 1999; Flaschke & Tranker, 1999). The other factors, like the linearity and sensitivity of a capacitive moisture sensor, are deeply dependent on the input frequency of the signal (Campbell, 1990; Balachander et al., 2021; Eller & Denoth, 1996).

Few capacitive soil moisture sensor designs were patented in 2007 and 2008. Their design can able to measure moisture at a particular depth quite efficiently. Davis et al., (2008) presented a design in which a processor and a memory are included in a system to measure soil moisture periodically. The design has two pluralities of electrodes embedded in a body with a sharp corner. These two pluralities of electrodes are imposed with a layer to protect from physical damage (Lee, 2007). The proposed model is made using Printed Circuit Board (PCB) technology. They designed the sensor probe by considering different parameters such as the thickness of the copper layer of the electrode (interdigital capacitive sensor), a gap of separation of two electrodes, base material, and deposited material properties. Complete hardware based on a fringing field capacitive sensor and the hardware model can measure soil moisture content and soil temperature for agricultural commodities (Mizuguchi et al., 2015; Dean et al., 2010).

In this research work, a study is carried out on three different types of interdigital sensor models for low-cost IoT-based agriculture applications. These three models are designed in COMSOL Multiphysics 5.4 and fabricated to use in an IoT-based soil moisture monitoring system. Sensor probes are fabricated using PCB Technology. Calibrated sensor probes are used in the sensing layer of IoT architecture to collect soil moisture data from the agriculture field. Figure 1 shows the use of a designed low-cost soil moisture monitoring system in the IoT layer. This low-cost portable system is designed around two microcontrollers. One microcontroller (W78E054D) generates a square wave of frequency 500 kHz and another IoT-enabled microcontroller (ESP8266) controls and processes the whole system.

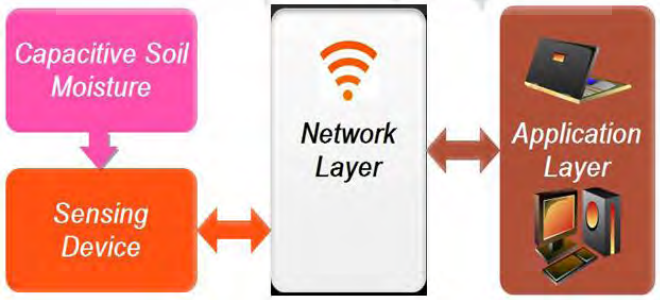

Figure 1. Block diagram of IoT architecture

Methodology

Design of capacitive moisture sensor

The existing soil moisture sensor probes cannot measure water content in the root zone (up to 30 cm) because of its small size. In this research, three different models of sensor probes are designed and calibrated to measure water content in the root zone. The dimension and structure of all three models, namely model A, B, and C, are shown in Figure 2. The total sensing area of each sensor is 10,800 cm2 (270cm×40cm). All these three sensor probes are based on the interdigital pattern. Two adjacent opposite polarity copper layer act as parallel plate capacitors. The total capacitance of the sensor probe is equal to the combination of all the parallel capacitors. The parallel capacitor's capacitance depends mainly on three factors, as evident from Equation (1).

$$C = \varepsilon \frac{A}{d} \quad (1)$$

Where ε = Permittivity of the dielectric medium, A = Area of capacitor plate, d=distance between two electrodes.

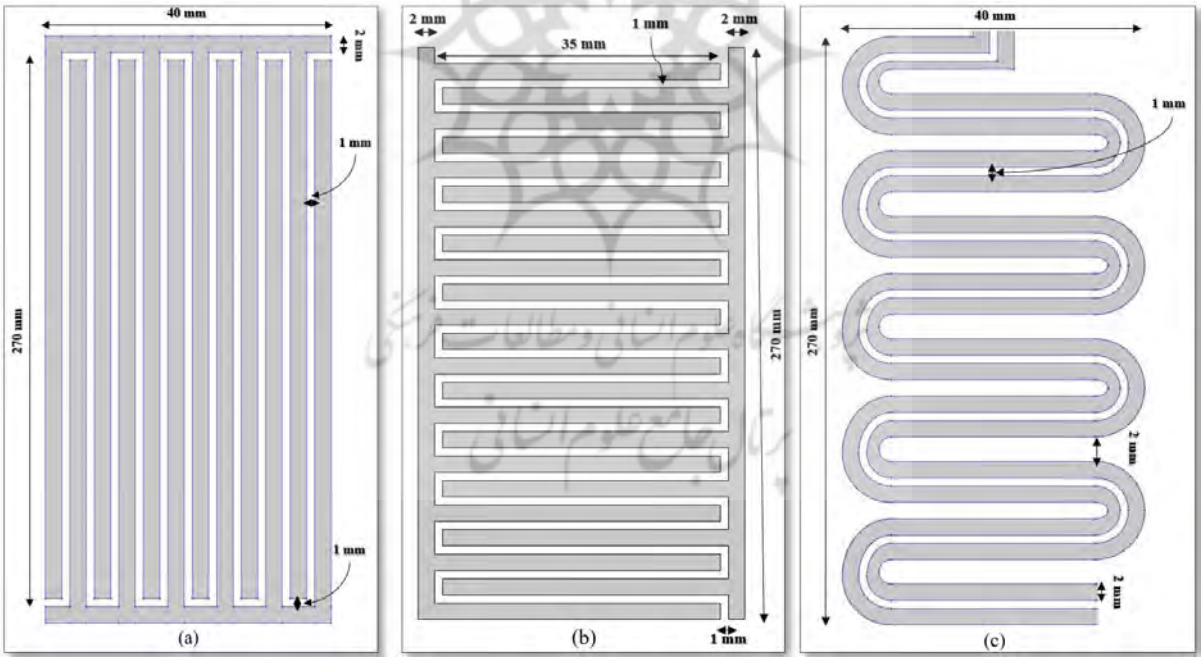

Figure 2. Structure and design of sensor probes (a) Model-A (b) Model-B (c) Model-C

So, all three models are designed in COMSOL Multiphysics 5.4 software by considering three factors: The Permittivity of the dielectric medium, the area of electrodes, and the gap between the two electrodes. A uniform potential distribution is also observed for the designed sensor probes, which are shown in Figure 3.

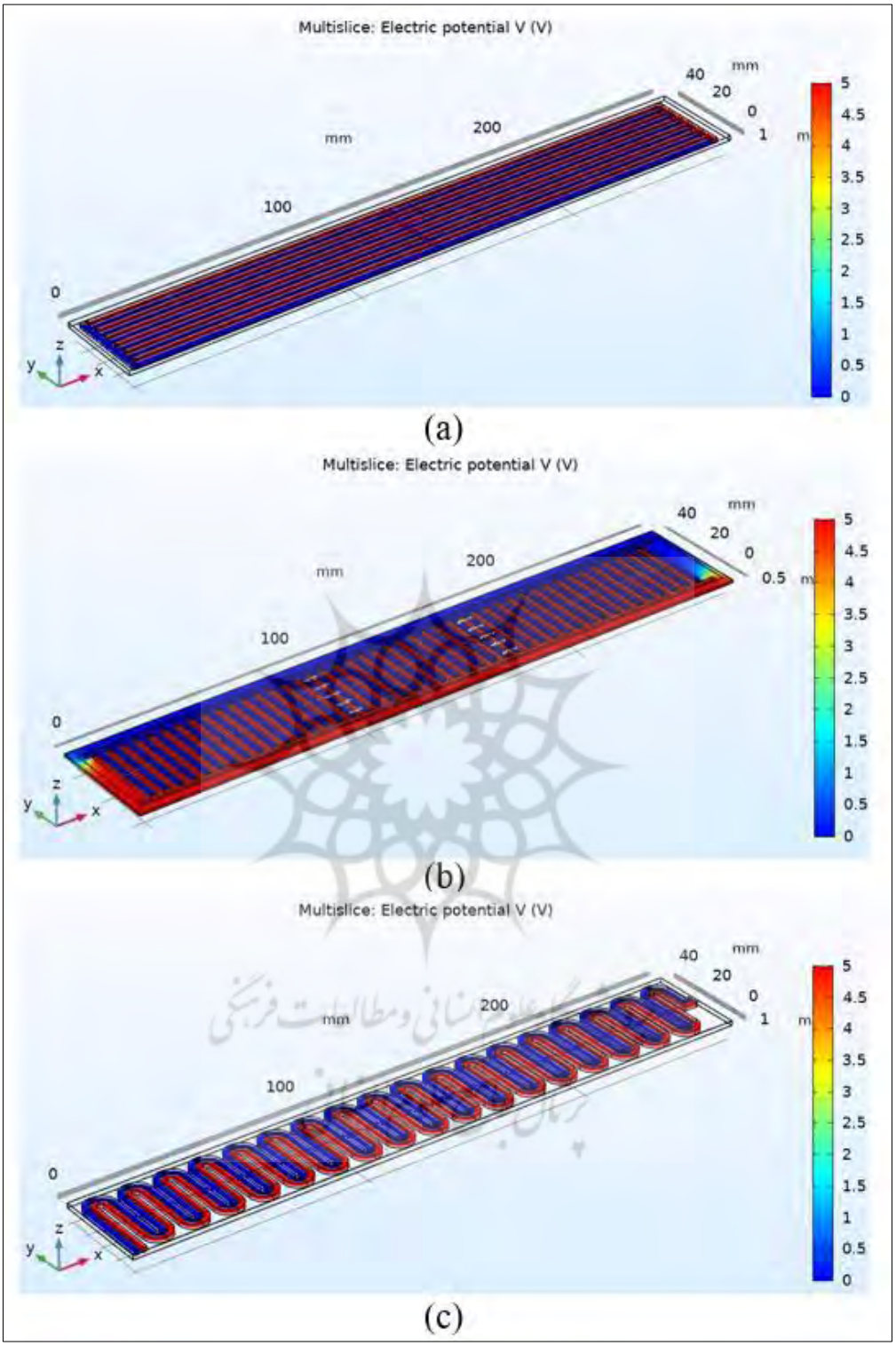

Figure 3. Potential distribution of design sensor probes (a) Model-A (b) Model-B (c) Model-C

The response of the capacitive sensor probes concerning the change of gap of two electrodes for different electrode areas is shown in Figure 4.

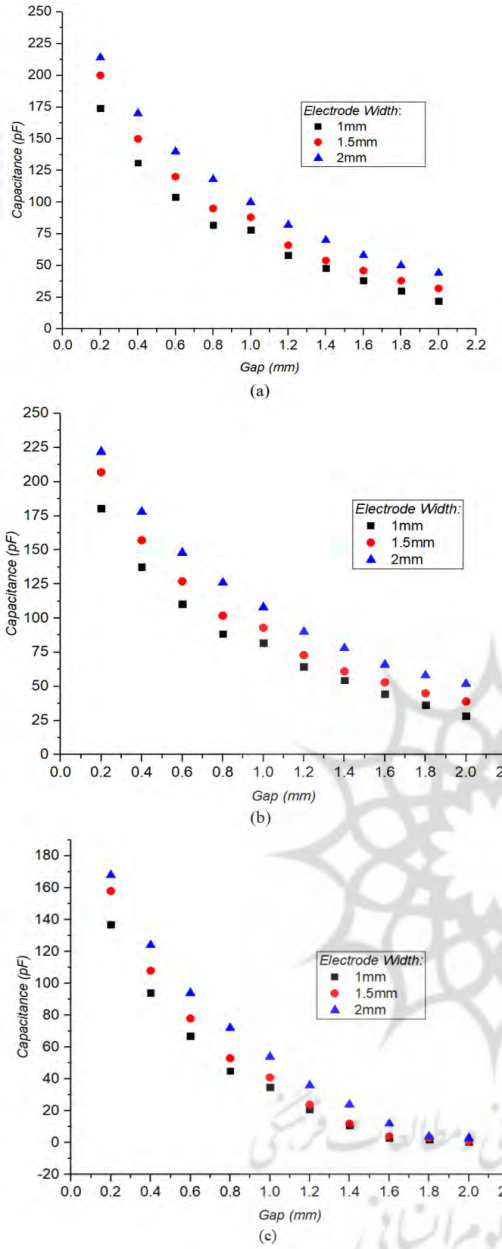

Figure 4. Response of capacitance Vs gap between two electrodes for (a) Model-A (b) Model-B (c) Model-C

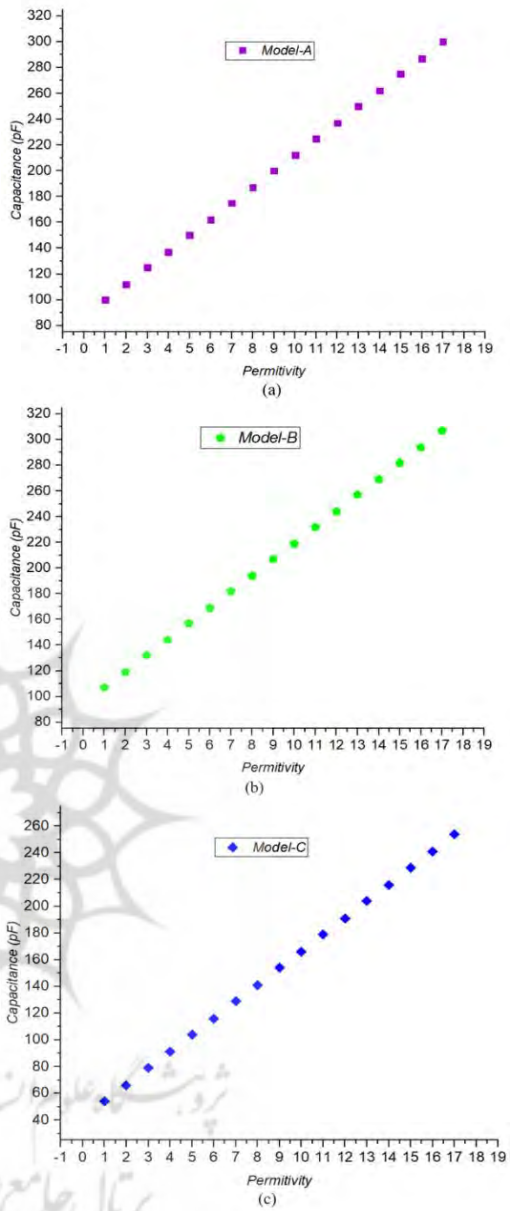

Figure 5. Response of capacitance Vs dielectric permittivity for (a) Model-A (b) Model-B (c) Model-C

From the response curve in Figure 4, it is clear that the capacitance increases with the increase of electrode area and decreases with the increase of the gap between two electrodes. Among the three designs, Model 3 has the lower output capacitance. The response of the designed sensor probe for the change of Permittivity is shown in Figure 5. A linear response is observed for all the designed sensor probes. In Table 1, linear characteristics of the sensor models for the change of dielectric Permittivity are shown.

Table 1. Linear characteristics response of the sensor models

Sensor probe	y-intercepts	Slopes	Goodness of fit
Model-A	87.26	12.5	1
Model-B	94.26	12.5	1
Model-C	41.26	12.5	1

All three models are fabricated using plain single-layer copper printed circuit board (PCB). The details of the PCB specification are mentioned in Table 2. The PCB layout is designed in Diptrace version 3.002 software and fabricated using Computerized Numeric Control (CNC) machine (Model: Accurate CNC A626, Software: PhCNC Pro v5.40.1.13501). All three fabricated sensor models are shown in Figure 6. After fabrication, an insulating layer of epoxy resin is applied to protect copper traces from any chemical reaction.

Table 2. Details of the PCB specification

Property	Type/Dimensions
Layer material	Glass fibre-reinforced epoxy Cu
The total thickness of the PCB	1.52 mm
The thickness of the Cu trace	0.0341 mm
The thickness of the board material	1.4659 mm
Substrate material	FR4
Withstand Voltage	24 V, DC
The resistivity of surface material	0.055 ohm

Figure 6. Fabricated sensor probes (a) Top view (b) Back view

Sensor system architecture

The architecture of the sensor system is shown in Figure 7. To make the soil moisture monitoring device ESP8266 controller is used to process the soil moisture parameter. The designed capacitive sensor probe is exited with a square wave signal with a frequency of 500

kHz. This frequency is generated using an 8051 series controller (W78E054DDG). The design sensor probe is connected to a signal converter circuit to read the change in the analogue voltage level. A rechargeable lithium-ion battery is used to power the system. A master switch is connected in series with the battery to control the ON/OFF action. An OLED display is also equipped to monitor the moisture value directly. The moisture value read by the system is sent to a server using the IoT enable controller. A mode select switch (reset switch) is interfaced to select the optimized calibrated Equation for a different type of soil (Silt/Sandy/Clay).

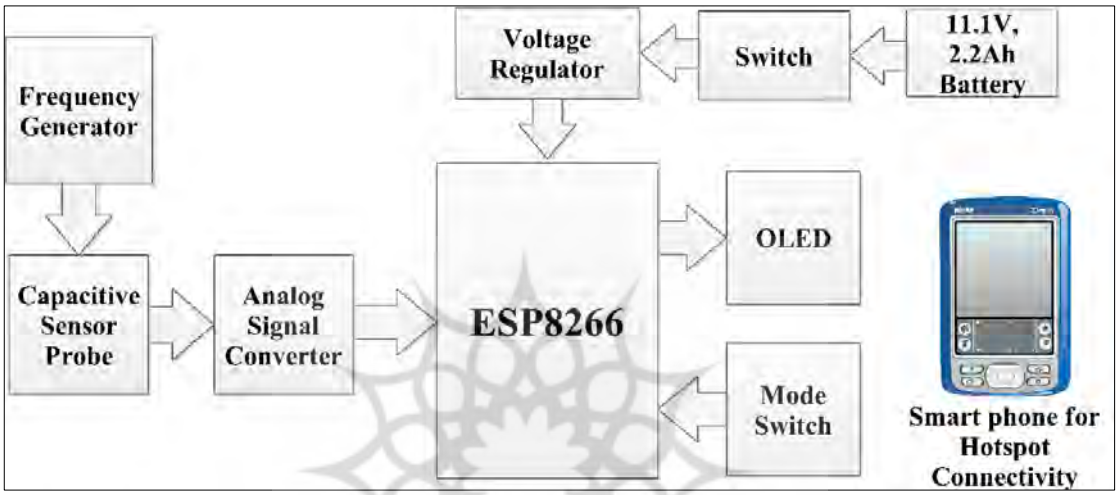

Figure 7. Proposed system architecture

Design of circuit diagram for sensor system

The circuit diagram to monitor the moisture content in the soil is shown in Figure 8. The 8051 series microcontroller W78054DDDG is a program to generate a square wave of frequency 500KHz with a duty cycle of 50%. TIMER 0 is programmed with the loaded value of (FFFE)H to generate a smooth square wave at the output. A crystal of 12 MHz is used to make the W78E054DDG functional. The square wave is generated at Port 2.0. The pin P2.0 is connected to one electrode of the sensor probe through a 10k resistor. The other electrode of the sensor probe is connected to the ground. This configuration works as an integrator to generate a triangular wave. This triangular wave charges up the output capacitor of 1 microfarad.

A 1 MΩ of the resistor is also connected in parallel to make a time constant of 1 second. A fast-switching diode 1N4148 is used in series to prevent the output capacitor from fully discharging when the output of the square wave goes low. The ADC of ESP8266 directly reads the captured analogue output. The OLED display is interfaced with ESP8266 using Serial Peripheral Interface (SPI) communication. A reset switch is connected at GPIO 6 to select the mode. This mode switch is used to provide a signal of high pulse to select the optimized calibrated Equation for soil.

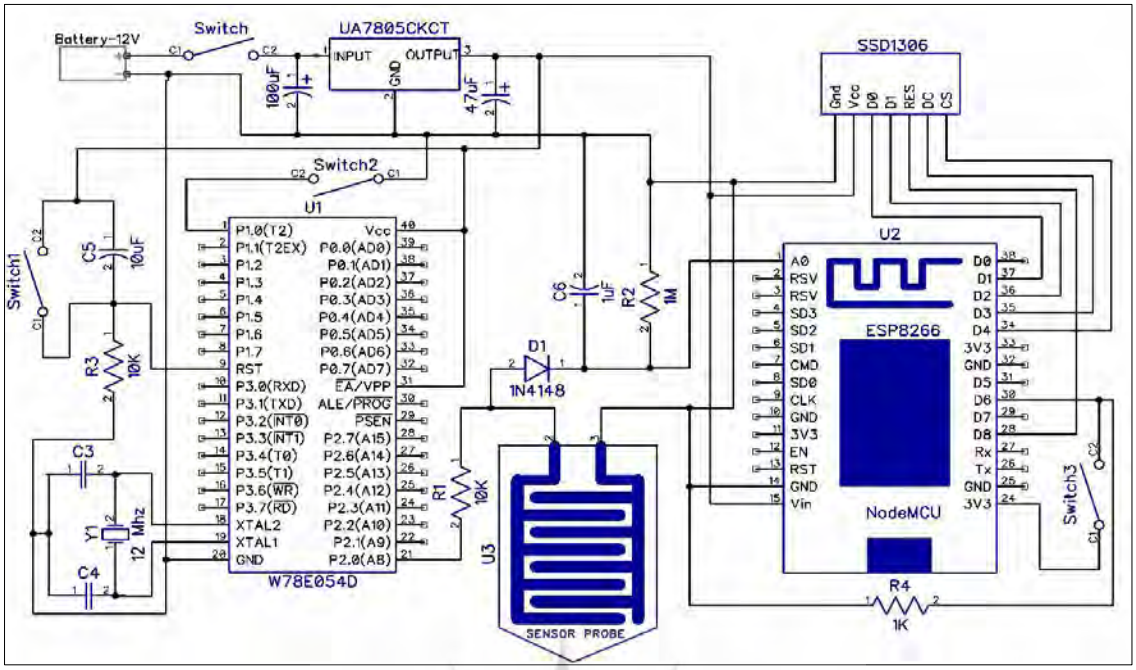

Figure 8. Electronic circuit diagram of the system

Design of hardware prototype model

A lightweight hardware model is presented in this research work. The model is designed to carry easily. The detailed structure and dimensions of the model are shown in Figure 9. The complete hardware model is the size of (39.8× 17.7) cm. To design the electronic system ESP8266 controller is preferred because this controller supports the IEEE802.11 communication protocol. 32-bit ESP8266 has many other features such as 32M bit of flash memory, inbuilt 10-bit analogue to digital converter (ADC), UART (universal asynchronous receiver-transmitter) connectivity, and support up to 160MHz of clock frequency. The other 8-bit W78E054DDG microcontroller has a program memory of 16 KB, 256B of SRAM, and maximum clock frequency support of up to 40MHz. The 128×64 OLED display supports SPI protocol to interface with any controller. The small display of size 0.96 inches is fitted on the top of the hardware model to read the moisture value.

An 11.1V, 2.2AH lithium-ion battery (SkyCell-RKI2733) is used to supply power. The battery has an inbuild protection circuit from overcurrent and overvoltage. The battery's rated charging and discharging currents are 1A and 4.4A, respectively. To charge up the battery, a 12V, 1A adapter is used. The battery takes around 47 minutes to fully charged. Figure 10 (a) shows all the required components to make the hardware prototype system. The circuit is assembled in a Vero board, as shown in Figure 10 (b). And the complete circuit is packed in a Polyvinyl chloride (PVC) box to make it fully waterproof. The complete hardware prototype device is shown in Figure 10 (c). to make the hardware prototype device; it costs INR1826.62 (25.20 USD). The complete components details used to design the soil moisture sensor system are shown in Table 3.

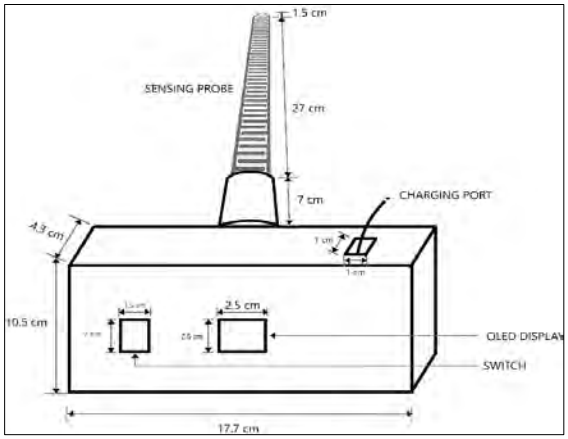

Figure 9. Structure and dimension of the prototype model

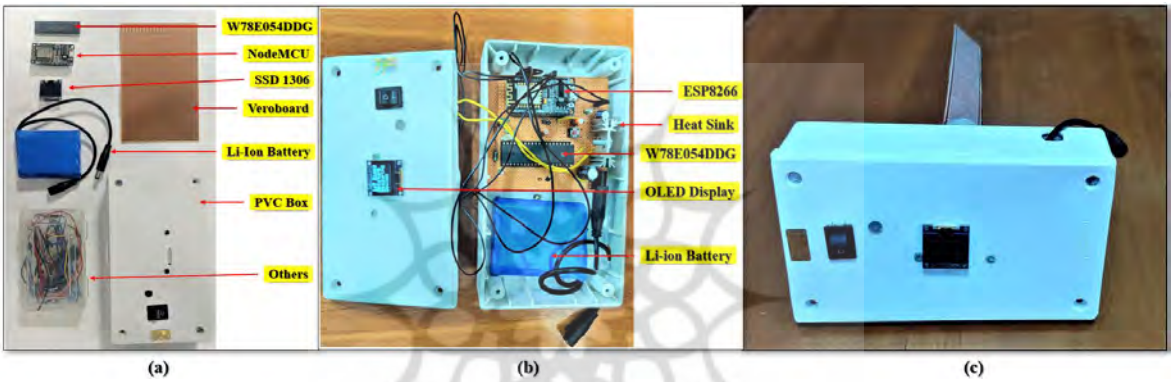

Figure 10. (a) Components to design the hardware model (b) Assembled electronic circuit (c) Hardware prototype device

Table 3. Components details used to design the soil moisture sensor system

Name	Model no.	Vendor	Cost (□)
Microcontroller	W78E054DDG	Nuvoton Technology	50.00
IoT enables development board	Node MCU	Espressif Systems	210.00
Voltage regulator 5V	UA7805CKCT	Texas Instrument	61.62
Li-Ion battery	RKI-2733	SkyCell	670.00
OLED display	SSD1306	WINSTAR	335.00
Other components	-	-	500.00
Total cost			1826.62

Results and Discussion

Three different types of soil are considered to calibrate the soil moisture sensor. Types 1, 2, and 3 are sandy soil, silt soil, and clay soil. These three types of soils are mainly considered because water holding capacity will vary with the soil types. Clay soil has a better water-holding capacity than silt and sandy soil. Since sandy soil particles are individual, sandy soil has less water-holding capability than the other soil types. The calibration process is carried out. (Borah et al., 2020). The output capacitance reading is taken using a RISH-Max digital multimeter (DMM) to change moisture content for three different soil types. The result of a change of capacitance for three different models and three different types of soil is shown in Figure 11.

The figure shows that the output capacitance value is more for Model B than the other two models for all three different types of soil. The response of capacitance of Model-C is minimum for all three types of soil. A linear fitting analysis is also done for the capacitance response, shown in Table 4. Table 4 shows that the goodness of fit for Model B is better than other presented models for all the types of soil except the silt soil. From the linear fitting analysis, it is also observed that the sensitivity of Model-A and Model B is almost the same. The response of output voltage concerning the change in moisture content is shown in Figure 12. The output voltage response is measured at the output of the analogue signal converter circuit using RISH series DMM. A linear fitting analysis for output voltage response is shown in Table 5. From the response data, it has been found that the performance of Model B in measuring moisture content for all the types of soil is better than the other two presented models.

Table 4. Linear fitting analysis for output capacitance response

Soil type	Models	Goodness of fit	Slope	Intercept
Sandy	Model-A	0.99894	21.32857 ± 0.31128	-73.28571 ± 13.92106
	Model-B	0.99993	21.03214 ± 0.07784	-21.71429 ± 3.481
	Model-C	0.99102	18.75 ± 0.79805	-164.28571 ± 35.68999
Silt	Model-A	0.99986	21.71429 ± 0.11535	-48.71429 ± 5.15871
	Model-B	0.99977	21.625 ± 0.14763	-6.85714 ± 6.60203
	Model-C	0.98828	19.08571 ± 0.92945	-160.28571 ± 41.56627
Clay	Model-A	0.99966	21.25714 ± 0.17659	-32.71429 ± 7.8973
	Model-B	0.99993	21.11429 ± 0.07706	8.85714 ± 3.44638
	Model-C	0.99045	18.86429 ± 0.82836	-139.57143 ± 37.0452

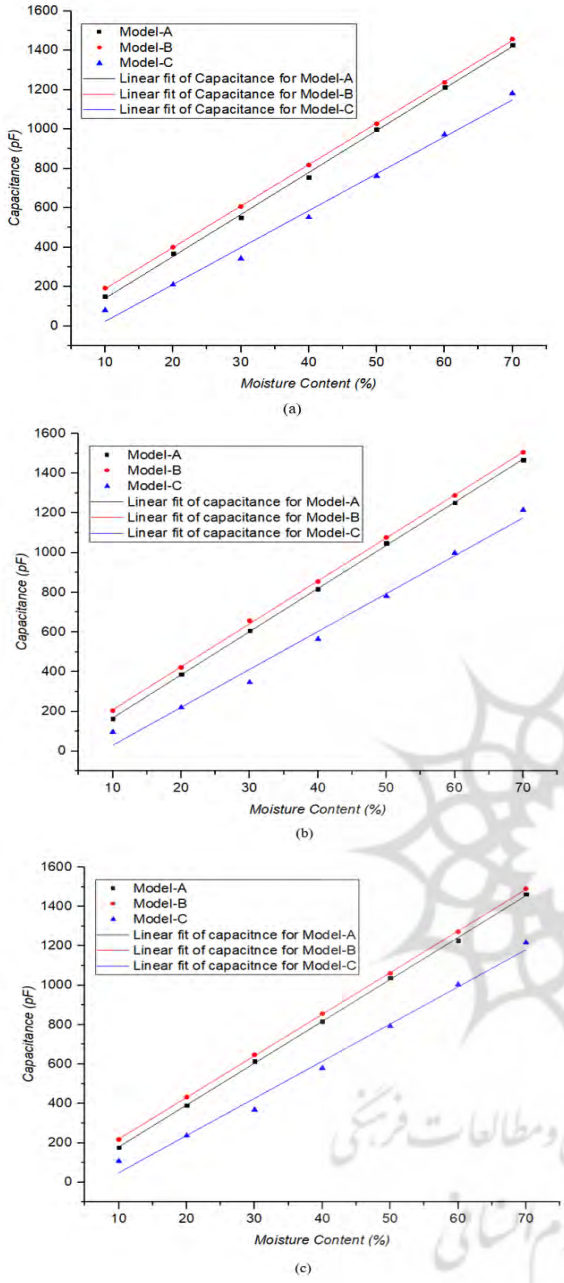

Figure 11. Response of capacitance Vs change of moisture content for (a) Sandy soil (b) Silt soil (c) Clay soil

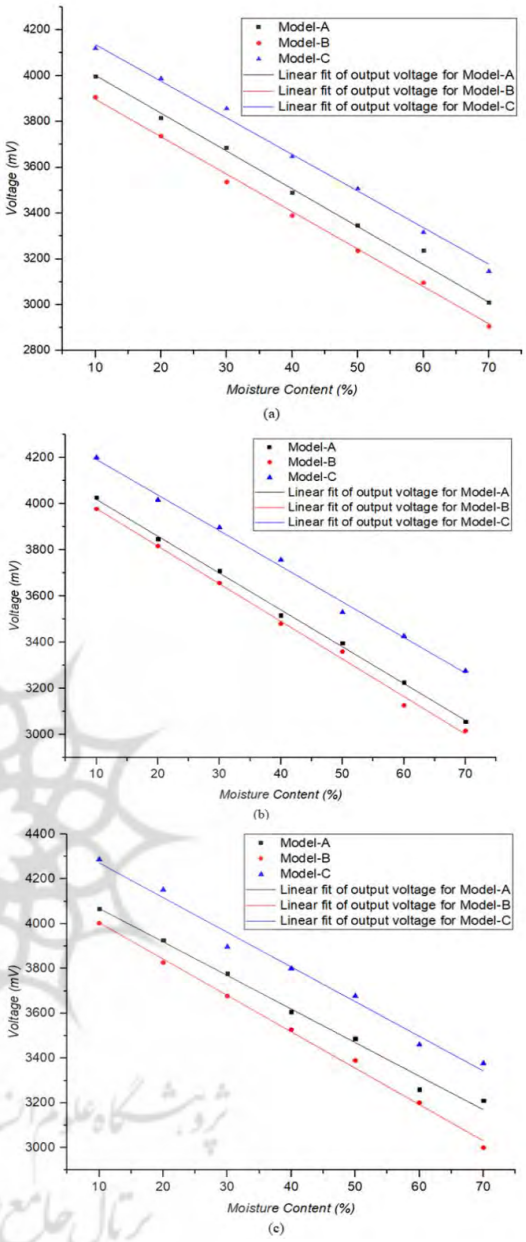

Figure 12. Response of output voltage Vs change of moisture content for (a) Sandy soil (b) Silt soil (c) Clay soil

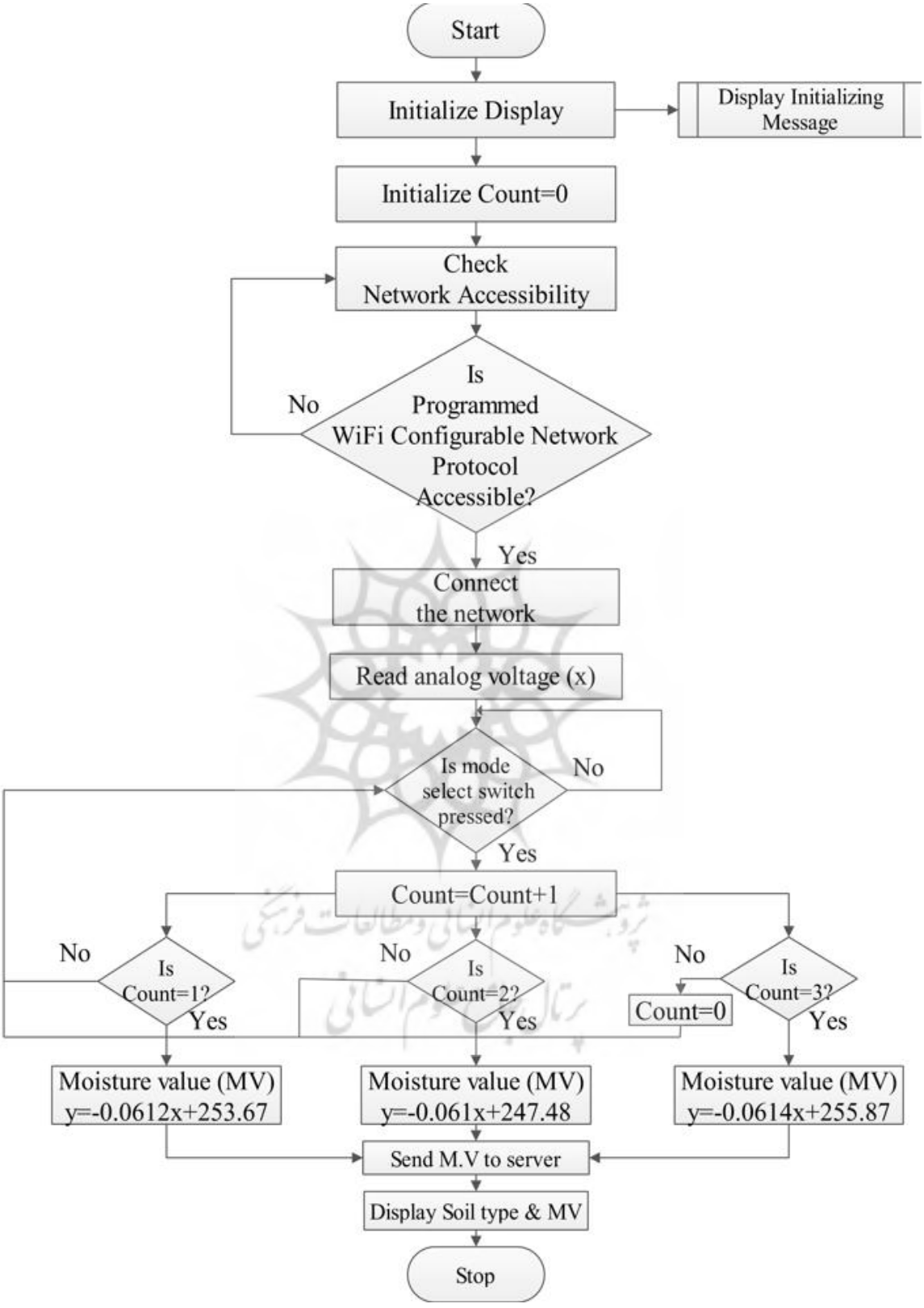

Figure 13. OMV algorithm flowchart

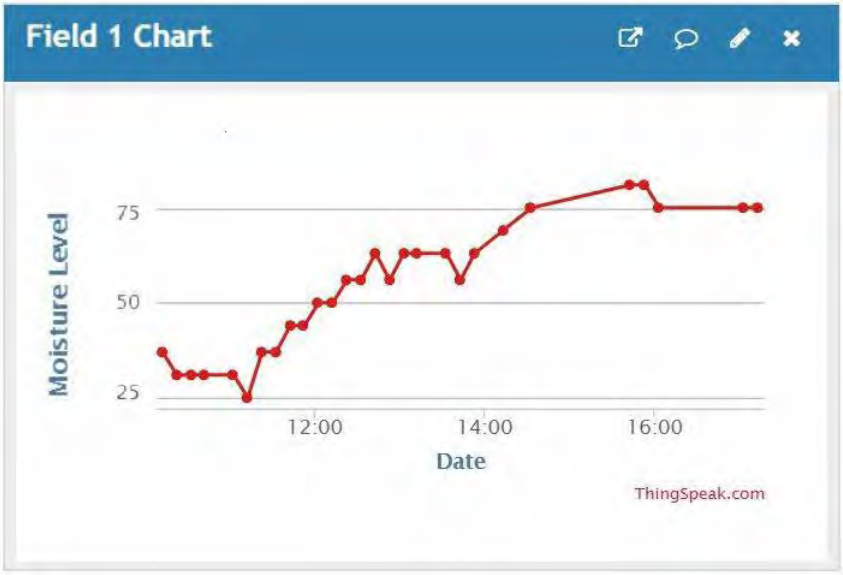

Figure 14. Received moisture data in the server

Table 5. Linear fitting analysis for output voltage response

Soil type	Models	Goodness of fit	Slope	y-intercept
Sandy	Model-A	0.99989	-16.50357 ± 0.07823	4166.57143 ± 3.49854
	Model-B	0.99982	-16.34286 ± 0.09918	4060.57143 ± 4.43548
	Model-C	0.99999	-15.97857 ± 0.01779	4295.57143 ± 0.79539
Silt	Model-A	0.99834	-15.93929 ± 0.2907	4177.85714 ± 13.00059
	Model-B	0.9962	-16.275 ± 0.44958	4141.71429 ± 20.10572
	Model-C	0.99459	-15.41429 ± 0.50856	4345.85714 ± 22.74347
Clay	Model-A	0.99092	-14.98214 ± 0.64146	4218.57143 ± 28.68682
	Model-B	0.99659	-16.23929 ± 0.42505	4167.14286 ± 19.00899
	Model-C	0.98685	-15.47857 ± 0.79918	4426.28571 ± 35.74028

From Figure 12, it is clear that the response of change of voltage to change in soil type varies significantly. So, an algorithm is developed to select the optimized calibration equation for a specific soil type. All the calibrated equations are derived from developing the OMV algorithm from the linear analysis of Model B. The calibrated Equations 2, 3, and 4 are for the silt, sandy, and clay soil. The controller of the electronic system is programmed according to the flowchart shown in Figure 13. The device can be configurable to other communication network protocols such as wireless sensor network (WSN) and WiMAX using peripherals. In this current work, inbuild WiFi IEEE 802.11 b/g/n protocol is used for communication. The WiFi-based communication network topology can be configurable to enhance communication with multiple systems.

The variable 'count' is initially considered 0 to select the soil type. This variable can be changed by using the mode select switch. When count = 0, the controller will be ready to find

the moisture value for silt soil. For count values 2 and 3, the device is ready to find the moisture value for sandy and clay soil. The device can be further configurable to measure soil moisture for peat soil, chalk soil, and loam soil by doing all the required calibrations. With all the soil moisture data from different soil types, a database can be made for future analysis of soil moisture for different agriculture fields of different soil types.

$$y=-0.0612x+253.67 \quad (2)$$

$$y=-0.0610x+247.48 \quad (3)$$

$$y=-0.0614x+255.87 \quad (4)$$

Where, y=Moisture value (%); x=Voltage (mV).

The historical moisture value in the server at a different time is shown in Figure 14. An open-source server thingspeak.com is used for this purpose.

Conclusion

Three sensor models, namely Model-A, Model-B, and Model-C, are designed and analyzed to make a handy device for measuring soil water content. The obtained result found that the response of capacitance and voltage for Model B with the moisture content change in the soil (sand/silt/clay) is better than the other two presented models. Sensor probes were fabricated using PCB technology, and an electronic system was developed to read the moisture value. The presented soil moisture device was controlled by developing an OMV algorithm to collect soil moisture data effectively. The OMV algorithm uses calibrated equations for effective moisture measurement based on the soil type. The obtained moisture readings were stored in a server for future analyses. The total cost to manufacture the hardware model is 1826.62 INR (24.82 USD).

Acknowledgements

The authors would like to thank the Technical Education Quality Improvement Program (TEQIP), Government of India, for providing a fellowship to carry out the research. The authors also like to thank the department of Electronics and Instrumentation Engineering, National Institute of Technology (NIT), Nagaland, for providing all the facilities to carry out the research.

Conflict of interest

The authors declare no potential conflict of interest regarding the publication of this work. In addition, the ethical issues including plagiarism, informed consent, misconduct, data fabrication and, or falsification, double publication and, or submission, and redundancy have been completely witnessed by the authors.

Funding

The author(s) received no financial support for the research, authorship, and/or publication of this article

References

Alessi R. S. and Prunty L. (1985), "Soil-water determination using fiber optics," Soil Sci. Soc. Amer. J., vol. 50, no. 4, pp. 860–863.

Balachander, K., Venkatesan, C., & Kumar, R. (2021). Safety driven intelligent autonomous vehicle for smart cities using IoT. International Journal of Pervasive Computing and Communications.

Bao X, Zhu X, Chang X, Wang S, Xu B and Luo C (2016), "Effects of Soil Temperature and Moisture on Soil Respiration on the Tibetan Plateau," PloS ONE, vol. 11, no. 10, pp. 1-14.

Borah S., Kumar R. and Mukherjee S. (2020), "Low-cost IoT framework to Control and Monitoring Irrigation," International Journal of Intelligent Unmanned Systems (IJIUS), vol. 9, no. 1, pp. 63-79.

Campbell J.E. (1990), "Dielectric properties and influence of conductivity in soils at one to fifty megahertz," Soil Sci. Soc. Am. J., Vol. 54, pp. 332-341.

Chen Z. and Luo R. C. (1998), "Design and implementation of capacitive proximity sensor using microelectromechanical systems technology," IEEE Trans. Ind. Electron., vol. 45, no. 6, pp. 886–894.

Curtis J. O. (2001), "Moisture effects on the dielectric properties of soils," IEEE Transactions on Geoscience and Remote Sensing, vol. 39, no. 1, pp. 125-128.

Davis S. C., Johnson P., Huberts J. (2008), Soil moisture sensor, US 20080199.359A1.

Dean R. N., Rane A., Baginski M., Hartzog Z., and Elton D. J. (2010), "Capacitive fringing field sensors in printed circuit board technology," in Proc. IEEE Instrum. Meas. Technol. Conf., Austin, TX, USA, pp. 970–974.

Eller H. and Denoth A. (1996), "A capacitive soil moisture sensor," J. Hydrol., vol. 185, nos. 1–4, pp. 137–146.

Evett S. R. and Steiner J. L. (1995), "Precision of Neutron Scattering and Capacitance Type Soil Water Content Gauges from Field Calibration," Soil Science Society of America Journal, vol. 59, no. 4, pp. 961-968.

Flaschke T. and Tranker H.-R. (1999), "Dielectric soil water constant measurements independent of soil properties," in Proc. 16th IEEE Instrum. Meas. Technol. Conf., Venice, Italy, pp. 37–41, May 24–26.

Huisman J. A., Hubbard S. S., Redman J. D., and Annan A. P. (2003), "Measuring soil water content with ground penetrating radar: A review," Vadose Zone J., vol. 2, pp. 476–491.

Langfelder G. and Tocchio A. (2012), "Differential fringe-field MSMS accelerometer," IEEE Trans. Electron Devices, vol. 59, no. 2, pp. 485–490.

Ledieu J., Ridder P. De, Clerck P. De and Dautrebande S. (1986), "A method of measuring soil moisture by time-domain reflectometry," Journal of Hydrology, Vol. 88, pp. 319–328.

Lee F. C. (2007), Capacitive soil moisture sensor, US7170302B2.

Lekshmi S. U. S., Singh D. N., and Baghini M. S. (2014), "A critical review of soil moisture measurement," Measurement, vol. 54, pp. 92–105.

Lin C.P. (2003), "Frequency domain versus travel time analyses of TDR wave-forms for soil moisture measurements," Soil Sci. Soc. Am. J., vol. 67, pp. 720–729.

Minet J., S., Lambot G. Delaide, Huisman J. A, Vereecken H., and Vanclooster M. (2010), "A Generalized Frequency Domain Reflectometry Modeling Technique for Soil Electrical Properties Determination", Vadose Zone Journal, vol. 9, no. 4, pp. 1063-1072.

Mizuguchi J., Piai J. C., França J. A. de, França M. B. de Morais, Yamashita K. and Mathias L. C. (2015), "Fringing field capacitive sensor for measuring soil water content: Design, manufacture, and testing," IEEE Trans. Instrum. Meas., vol. 64, no. 1, pp. 212–220.

Raats P. A. C. and Van Genuchten M. T. (2006), "Milestones in soil physics," Soil Sci., vol. 171, pp. S21–S28.

Rao B. and Singh D. N. (2011), "Moisture content determination by TDR and capacitance techniques: A comparative study," Int. J. Earth Sci. Eng., vol. 4, no. 6, pp. 132–137.

Ritchey L. W. (1999), "A survey and tutorial of dielectric materials used in the manufacture of printed circuit boards," in Proc. PCB Design Conf. West, Santa Clara, CA, pp. 1–10.

Scott C. A., Bastiaanssen W. G. M, and Ahmad M. D. (2003), "Mapping Root Zone Soil Moisture Using Remotely Sensed Optical Imagery," Journal of Irrigation and Drainage Engineering, vol. 129, no. 5, pp. 326–335.

Tang Chunling and Chen Dong (2017), "Interaction between Soil Moisture and Air Temperature in the Mississippi River Basin," Journal of Water Resource and Protection, vol. 9, no. 10, pp. 1119-1131.

Thamaraimanalan, T., Mohankumar, M., Dhanasekaran, S., & Anandakumar, H. (2021). Experimental analysis of intelligent vehicle monitoring system using Internet of Things (IoT). EAI Endorsed Transactions on Energy Web, 8(36).

Uddin Zahoor, Jantad Saowapa and Boonsupthip Waraporn (2016), "Effect of air temperature and velocity on moisture diffusivity in relation to physical and sensory quality of dried pumpkin seeds," Drying Technology international journal, 34 (12), pp. 1423-1433.

Zazueta F.S., Xin J. (1994), "Soil Moisture Sensors," Florida Cooperative Extension Service, Bulletin 292, Inst. Food and Agricultural Sciences, University of Florida, Gainesville.

Bibliographic information of this paper for citing:

Siddhanta, Borah; Kumar, R. & Subhradip, Mukherjee (2023). Design and Characterization of a Low-Cost Capacitive Soil Moisture Sensor System for IoT Based Agriculture Applications. *Journal of Information Technology Management*, 15 (Special Issue), 95-111. https://doi.org/10.22059/jitm.2023.91570